

## CO3-1 Local Two-phase Flow Characteristics for 6x6 Rod Bundle Geometry

Xiuzhong Shen, Shuichiro Miwa<sup>1</sup>, and Yigeng Xiao<sup>1</sup>

*Institute for Integrated Radiation and Nuclear Science,  
Kyoto University*

<sup>1</sup>*Faculty of Engineering, Hokkaido University*

**INTRODUCTION:** The rod bundle two-phase flow is a commonly utilized configuration for nuclear reactor fuel assembly. In the state-of-the-art, the accuracy of the two-fluid model, the most comprehensive and detailed formulation to describe two-phase flow behavior, is heavily dependent on the constitutive equations to close their interfacial transfer terms. In order to develop reliable constitutive equations for rod bundle geometry, understanding of the local flow parameters and their profiles which describe their gas-liquid interaction behaviors is indispensable. In the current joint project between Kyoto University and Hokkaido University, adiabatic air-water two-phase flow experiment using 6×6 rod bundle geometry was carried out. The local void fraction, interfacial area concentration (IAC) and interface velocity were measured using in-house made double-sensor probe, which was manufactured using optical-fiber probe. The bubbly flow regime was selected for the test condition to investigate the phase distribution of the bubbles in spherical and distorted particle regimes. At a cross section of the rod-bundle test section in several axial locations, 16 measurement points were selected in the octant symmetric triangular zone.

**EXPERIMENTS:** The schematic of the test section utilized in the current project is shown in Fig. 1, which is located in the Institute for Integrated Radiation and Nuclear Science of Kyoto University. In order to visualize the flow behavior, the test section was made of transparent acrylic square duct with a cross-section of 100 mm x 100 mm casing. 36 aluminum rods with diameters of 10 mm were inserted inside the test section to form a 6 x 6 rod bundle geometry. These rods were placed 16.7 mm pitch length apart. The hydraulic diameter ( $D_H$ ) of the test section was 18.7 mm and the overall height of the test section was 3 m. In order to prevent the vibration and unwanted flow disturbances, simplified spacer grids were installed at 4 different axial locations. These spacer grids also represent the actual spacer utilized in the light water reactor. The purified water was supplied from the centrifugal pump attached to the water tank and its volumetric flow rate was monitored by the electromagnetic flow meter. The compressed air was supplied from the air-compressor and its flow rate was monitored using mass-flow meter. They are injected into the mixing chamber located at the inlet section and well-mixed two-phase flow was injected into the test section. Pressure transducers as well as thermocouples were utilized to constantly monitor the axial pressure drop and fluid temperature for the determination of accurate physical parameters.

In the current phase of the project, the local flow parameters were measured using double-sensor optical probe.

Measurements at 16 different positions at the axial location ( $z$ ) of  $z/D_H=149$  were successfully conducted. Both core-peaking and wall-peaking phenomena were observed, depending on the flow conditions. For the data processing, the double-sensor probe algorithm as well as interface-pairing scheme developed by the previous researchers were adopted [1]. In order to convert the local parameters into the area-averaged value, the method proposed by Yang et al. [2] was adopted. According to the methodology, the conversion coefficients of the subchannel center and the rod gap values were determined as 0.662 and 0.243, respectively, for core-peaking profiles and 0.479 and 0.430 respectively for wall-peaking profiles.

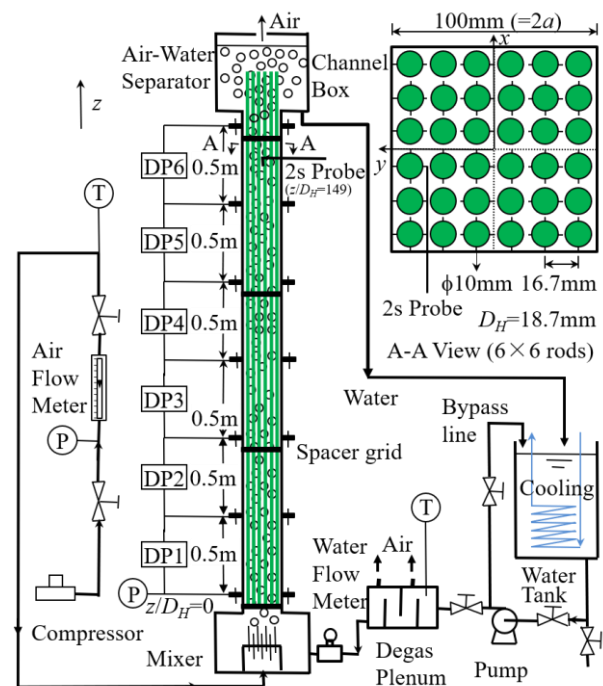


Fig. 1. 6x6 Rod Bundle Test Section [1]

**RESULTS:** For the local parameters obtained in the experiment, typical core-peaking and wall-peaking profiles in radial direction were confirmed in the present flow conditions. It was also found that the measured parameters in the rod gaps were much smaller than those in the center-region of the sub-channel. Based on the currently established area-averaged void fraction and IAC database, the drift-flux model and an IAC correlation were utilized to examine their accuracy, respectively. It was found that these models are capable of estimating the current experiment within 14.5% and 22.2% error, respectively.

### REFERENCES:

- [1] X. Shen *et al.*, *Exp.Comp.Multiph. Flow*, (2019) (In Press).
- [2] Yang, X. *et al.*, *Int. J. Heat Fluid Fl.*, Vol. 34, 85-97 (2012).

## CO3-2 Basic Research for Sophistication of High-power Reactor Noise Analysis

S. Hohara<sup>1</sup>, A. Sakon<sup>1</sup>, K. Nakajima<sup>2</sup>, K. Takahashi<sup>2</sup>, K. Hashimoto<sup>1</sup>

<sup>1</sup>Atomic Energy Research Institute, Kindai University

<sup>2</sup>Interdisciplinary Graduate School of Science and Engineering, Kindai University

**INTRODUCTION:** Reactor noise for high-power reactors were actively measured in the 1960's and 1970's. The major focuses of those researches were for the abnormality diagnosis or the output stabilization diagnosis, and almost researchers were in the field of system control engineering or instrumentation engineering. High-power reactor noise measurements for dynamics' analysis of reactivity change, reactivity feedback or reactor characteristics itself were few in the time (1960's and 1970's), because of the powerless measurement system. In this research, we plan to measure KUR's output with present-day measurement system and plan to analyze with several analysis methods. The results of this work will supply some knowledges and technics in the aspect of sophistication of reactor noise analysis or simulation methods.

In this year, we tried to measure the reactor nuclide noise of the critical & subcritical state KUR core via the fission chambers which installed into the KUR control console. The experimental work was done in 30 January 2018, 13 – 14 September 2018 and in 2 October 2018. In the analysis of the experimental results, we found that some external electrical noises were inserted into the fission chambers' signals. The noises have bad effect on the analysis results of the reactor noise, and in some case, the noises cannot be separated from the reactor nuclide noise signals. The situation of the external electrical noise on the KUR control console's fission chamber line is reported in this paper.

**EXPERIMENTS:** In this experiment, the output signal was lined from the control console of KUR. The target signal was of the fission chamber #1 & #2. The signal was binarized in the control console as a 4V/0.5  $\mu$  sec-TTL signal. The signal was measured a time-series measurement system (HSMCA4106\_LC: ANSeeN Inc.). A schematic view of the measurement is shown in Fig. 1.

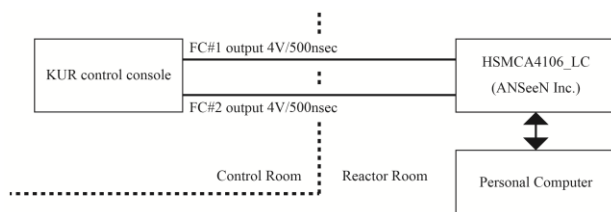


Fig. 1. Schematic view of the measurement.

The experimental condition is shown in Table.1. The criticality was set from -2.9%  $\Delta k/k$  to critical state. No.1

– 3 were run on 30 January 2018, No. 4 were run on 13 – 14 September 2018 and No.5-10 were run on 2 October 2018. The restrictions of the reactor room IN/OUT were set on No.4-10.

Table 1. Experimental condition

No.	Criticality [% $\Delta k/k$ ]	Measurement Time [sec]	Restrictions of Reactor Room IN/OUT
1	$\approx -2.9$	7,200	×
2	$\approx -2.9$	1,800	×
3	$\approx -2.9$	1,400	×
4	$\approx -2.9$	3,160	○
5	-2.949	3,600	○
6	-2.100	3,600	○
7	-1.153	1,800	○
8	-0.619	1,800	○
9	-0.326	1,800	○
10	0 (0.3W)	600	○

**RESULTS:** The external noise incident was separated from the normal reactor noise by observing the msec order count rate data of each experimental result.

The number of the external noise incident is shown in Table 2. In No.10, the external noise incident cannot be separated from the reactor noise because of the high-count rate of the reactor noise itself.

From the result, it can be founded that the number of external noise incident is strongly related to the restrictions of reactor room IN/OUT. This shows that the external noise on KUR control console occurs with the operation of the reactor room door's interlock circuit or neighbor peripherals.

Generally, the noise link of different circuits is a result of the close connection of power line or ground line. The KUR control console power/ground line should be separated from the other peripherals to keep the control monitors clear from other noise sources. At least, the KUR control console detectors in the present situation are not suitable for the pulse-mode reactor noise measurement.

Table 2. The number of the external noise incident

No.	Number of Ext. Noise Incident	Ext. Noise Incident Rate [/hour]
1	3	1.5
2	4	8
3	3	7.7
4	0	0
5	2	2
6	0	0
7	0	0
8	1	2
9	0	0
10	—	—

### CO3-3 Development of In-reactor Observation System Using Cherenkov Light (VIII)

T. Takeuchi, K. Yamamoto\*, Y. Namekawa, N. Takemoto, K. Tsuchiya, T. Sano<sup>1,\*\*</sup>, H. Unesaki<sup>1</sup>, Y. Fujihara<sup>1</sup>, Y. Takahashi<sup>1</sup> and K. Nakajima<sup>1</sup>

Waste Management and Decommissioning Technology Development Center, JAEA

<sup>1</sup>Institute for Integrated Radiation and Nuclear Science, Kyoto University

\* Current affiliation: Nuclear Engineering Co., Ltd.,

\*\* Current affiliation: Kindai University Atomic Energy Research Institute

**INTRODUCTION:** On-line surveillance system which can visualize and quantitatively evaluate reactor statuses will contribute to reactor operation management. Development of an on-line reactor core imaging system using Cherenkov light started in 2009. Previously, reactor power of the KUR was successfully estimated from brightness Cherenkov light using a commercial CCD camera<sup>[1]</sup>. In this study, in order to assess of a developing Cherenkov light analyzing system, a long- and real-time estimation of the reactor power by the system was performed.

**EXPERIMENTS:** The CCD camera (AEC-100ZL, Q-I Inc.) was inserted into core-observation pipe of KUR during starting up, keeping the power at 5 MW, and shutting down. The output of the CCD camera had been collected as a movie file and it was used to real-time estimate the reactor power by a developing Cherenkov light analyzing system. Figure 1 shows the setting screen of the system, which was set to obtain the image brightness due to Cherenkov light in the area not overlapping with characters was obtained in real time. The conversion factor from brightness to reactor power was determined assuming that the brightness reached maximum at 5 MW.

**RESULTS:** Figure 2 shows the comparison of the reactor thermal power from the control system measure value and the estimated value by Cherenkov light. At the reactor start up, the image brightness by Cherenkov light corresponded well to the change of the reactor thermal power. During 5MW, the image brightness showed the

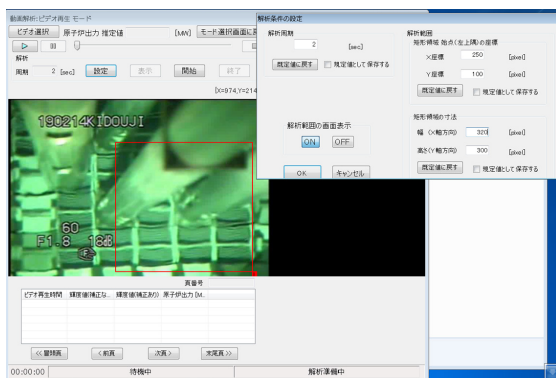


Fig. 1. The setting screen of the Cherenkov light analyzing system. The inside of the red border is analysis area.

behavior of gradually decreasing followed by recovering rapidly several times. After the shutdown, the image brightness decreased more gently than the heat output and showed a hunting-like phenomenon once. The gentle decrease is to be due to the Cherenkov light by radioactive decay of fission products remaining after reactor shutdown. On the other hand, as shown in fig. 2, the drop followed by recovery at 5 MW and the hunting after shutdown were found to be due to the adhesion of air bubbles followed by their detachment and the in-core cable, respectively.

**CONCLUSION:** As part of the development of the visible on-line core surveillance system, a long- and real-time estimation of the thermal power by brightness of Cherenkov light was performed in trial. As a result, It is found that it is necessary to consider the removal of the influence of air bubbles and reactor internals and the influence of FP on the image brightness.

**REFERENCES:**

[1] N. Ohtsuka, *et al.*, KURRI Progress Report 2013 (2015), P. 215.

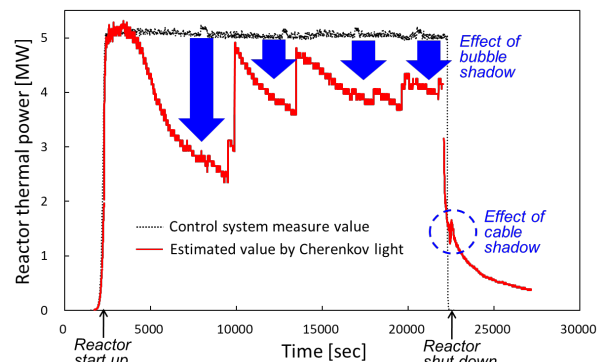


Fig. 2. The comparison of the reactor thermal power from the control system measure value and the estimated value by Cherenkov light.

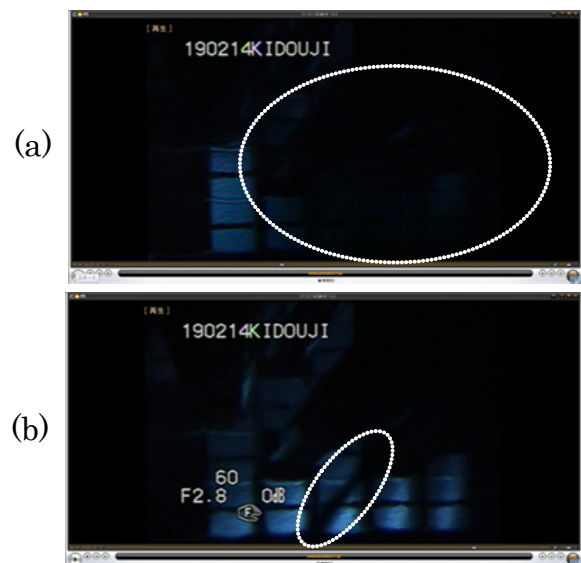


Fig. 3. The shadow of (a) bubble and (b) cable indicated by white dotted circles

# CO3-4 Measurements of $\beta_{eff}/\Lambda$ in Accelerator-Driven System with 14 MeV Neutrons

C. H. Pyeon<sup>1</sup>, M. Yamanaka<sup>1</sup>, D. J. Lee<sup>2</sup> and H. J. Shim<sup>3</sup>

<sup>1</sup> Institute for Integrated Radiation and Nuclear Science, Kyoto University (KURNS)

<sup>2</sup> Department of Nuclear Engineering, Ulsan National Institute of Science and Technology (UNIST), Korea

<sup>3</sup> Department of Nuclear Engineering, Seoul National University, Korea

**INTRODUCTION:** The polyethylene-moderated (solid-moderated) core (A-core) has been designed at Kyoto University Critical Assembly (KUCA) for a subcritical reactivity estimation experiment. The accelerator-driven system (ADS) experiments were carried out at the A-core with 14 MeV neutrons, to estimate  $\beta_{eff}/\Lambda$  value with the combined use of reactivity in dollar units ( $\rho_s$ ) and prompt neutron decay constant ( $\alpha$ ) values obtained by the pulsed-neutron source (PNS) method and the Feynman- $\alpha$  method, respectively. At a near critical state, the value of  $\beta_{eff}/\Lambda$  was experimentally obtained with an injection of 14 MeV neutrons into the A-core, and examined soundly with the consideration of dependence of measured results on the detector position and kind.

**EXPERIMENTS:** The core configuration of ADS experiments with 14 MeV neutrons is shown in Fig. 1. “F” is a normal fuel assembly composed of uranium and polyethylene, and “p” is a polyethylene moderator assembly. Subcriticality was attained by full withdrawal of all control (C1, C2 and C3) and safety (S4, S5 and S6) rods from the core, and experimentally deduced by the PNS method (extrapolated-area ratio method): about 80 pcm. The characteristics of pulsed-neutron beams were as follows: 0.1 mA current, 20 Hz pulsed repetition and 97  $\mu$ s pulsed width.

**RESULTS:** Experimental results were summarized as shown in Table 1. The values of  $\alpha$  [1/s] and  $\rho_s$  [\$] were obtained by the Feynman- $\alpha$  (Fig. 2) and the PNS methods, respectively. Moreover, with the combined use of  $\alpha$  and  $\rho_s$ ,  $\beta_{eff}/\Lambda$  was deduced experimentally by the  $\alpha$ -fitting method. As shown in Table 1, objective values of  $\beta_{eff}/\Lambda$  were observed remarkably to be valid at near critical state (80 pcm), although somewhat depending on the location of detector.

Table 1. Measured results of  $\beta_{eff}/\Lambda$  [1/s]

Detector	$\alpha$ [1/s]	$\rho_s$ [\$]	$\beta_{eff}/\Lambda$ [1/s]
BF-3 #1	$319.2 \pm 71.6$	$0.023 \pm 0.007$	$288.2 \pm 93.3$
BF-3 #2	$364.0 \pm 75.7$	$0.016 \pm 0.005$	$223.4 \pm 79.5$
BF-3 #3	$270.4 \pm 13.9$	$0.019 \pm 0.003$	$253.7 \pm 37.3$
Fiber #1	-	$0.021 \pm 0.006$	$243.4 \pm 72.1$
Fiber #2	$268.8 \pm 20.7$	$0.020 \pm 0.003$	$225.4 \pm 383.$
Fiber #3	$310.4 \pm 43.0$	$0.026 \pm 0.006$	$267.0 \pm 62.6$

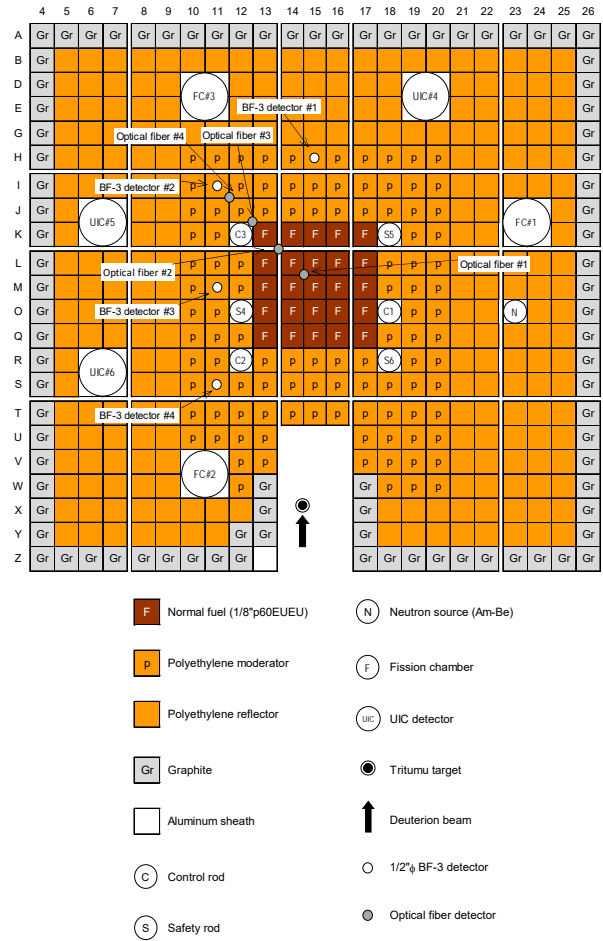


Fig. 1. KUCA core configuration

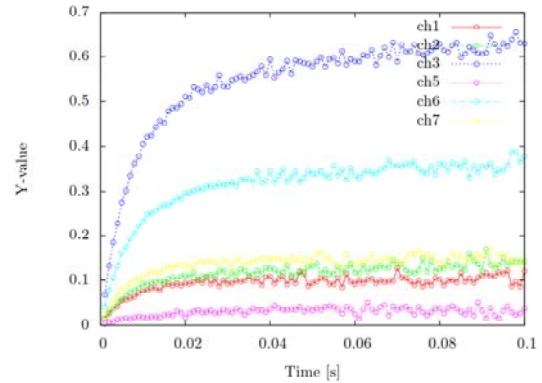


Fig. 2. Feynman- $\alpha$  fitting results

**ACKNOWLEDGEMENT:** This research was conducted under the International Collaboration Research between UNIST, Korea and Institute for Integrated Radiation and Nuclear Science, Kyoto University.

# CO3-5 Transient Analyses of Kinetics on Accelerator-Driven System with 14 MeV Neutrons

C. H. Pyeon and M. Yamanaka

Research Center for Safe Nuclear System,  
Institute for Integrated Radiation and Nuclear Science,  
Kyoto University

**INTRODUCTION:** The Kyoto University Critical Assembly (KUCA) has a polyethylene-moderated (solid-moderated) core (A-core), and the accelerator-driven system (ADS) experiments were carried out at the A-core with 14 MeV neutrons, to monitor transients (Fig. 1) of kinetic parameters in time evolution with an injection of 14 MeV neutrons. To estimate prompt neutron decay constant ( $\alpha$ ), the pulsed-neutron source (PNS) and the Feynman- $\alpha$  method were applied to the ADS experiments.

**EXPERIMENTS:** The core configuration of ADS experiments with 14 MeV neutrons is shown in Fig. 2. Normal fuel “F” is a normal fuel assembly composed of uranium and polyethylene, and “p” is a polyethylene moderator assembly. Subcriticality was attained by full insertion of C1 control rod into and full withdrawal of control (C2 and C3) and safety (S4, S5 and S6) rods from the core, and experimentally deduced by the PNS method (extrapolated-area ratio method): about 1474 pcm ( $k_{eff} = 0.985$ ). The characteristics of pulsed-neutron beams were as follows: 0.1 mA current, 20 Hz pulsed repetition and 97  $\mu$ s pulsed width. Transient behavior of neutron counts in the time evolution ranging between 1300 and 2800 s, as shown in Fig. 1.

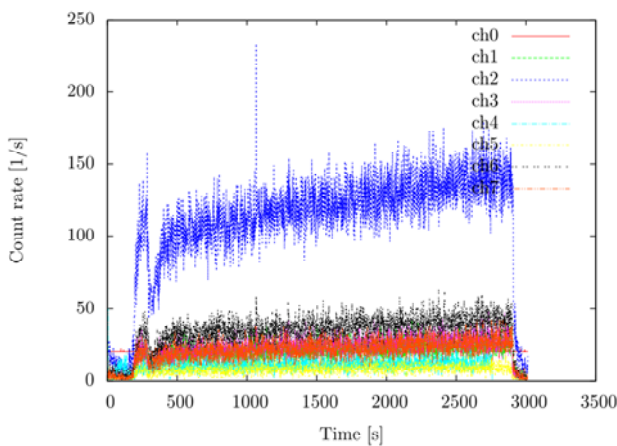


Fig. 1. Neutron counts with beam transients in time evolution ranging between 1300 and 2800 seconds

**RESULTS:** Experimental results were summarized as shown in Table 1. The values of  $\alpha$  [1/s] were obtained by the PNS and the Feynman- $\alpha$  methods. As shown in Table 1, the  $\alpha$  values by the two methods were observed to be

valid at subcriticality level  $k_{eff} = 0.985$ , and resulted approximately in no difference between the measurement methodologies, within an allowance uncertainty. Also, the  $\alpha$  values were found remarkably to be independent of detector positions, with in a relative difference of 5%, as shown in Table 1.

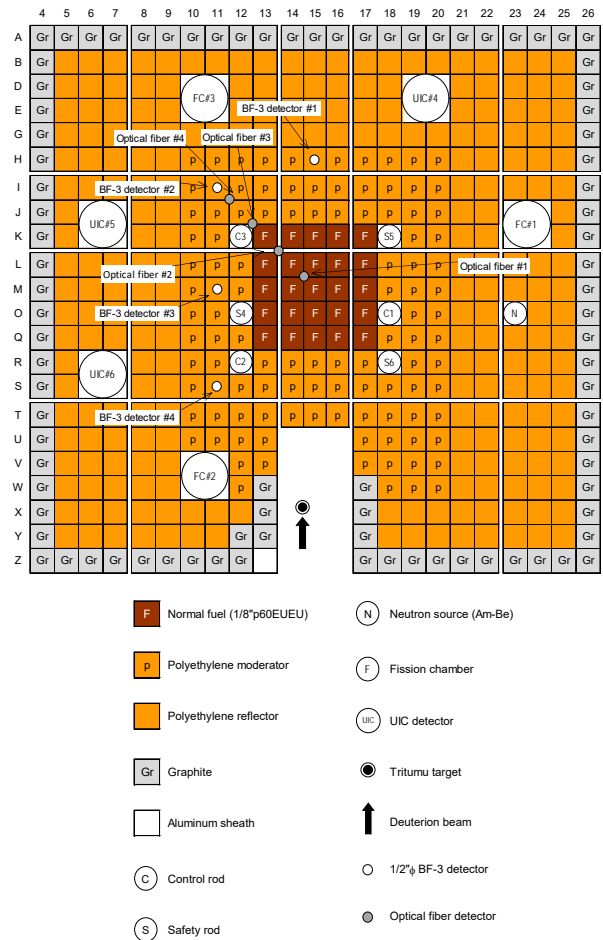


Fig. 2. KUCA core configuration with ADS experiments with 14 MeV neutrons

Table 1. Measured results of  $\alpha$  values [1/s]

Detector	PNS method	Feynman- $\alpha$ method
BF-3 #1	$528.3 \pm 9.0$	$511.7 \pm 7.9$
BF-3 #2	$528.9 \pm 8.2$	$525.5 \pm 6.5$
BF-3 #3	$532.6 \pm 3.4$	$524.6 \pm 2.7$
Fiber #1	$551.6 \pm 16.0$	$519.0 \pm 15.3$
Fiber #2	$531.1 \pm 6.6$	$535.6 \pm 5.6$
Fiber #4	$538.8 \pm 7.9$	$524.4 \pm 7.7$

# CO3-6 Data assimilation using subcritical measurements: reactor-noise measurement under the shutdown state, and transient experiments for source driven subcritical system

T. Endo<sup>1</sup>, K. Watanabe<sup>1</sup>, T. Ikeda<sup>1</sup>, A. Nonaka<sup>1</sup>, T. Sano<sup>2</sup>, M. Yamanaka<sup>2</sup>, C.H. Pyeon<sup>2</sup>

<sup>1</sup>Graduate School of Engineering, Nagoya University

<sup>2</sup>Institute for Integrated Radiation and Nuclear Science, Kyoto University

**INTRODUCTION:** In a general transient in a subcritical system, reactivity, neutron source intensity  $S$ , and point kinetic parameters ( $\Lambda$  and  $\beta_{\text{eff}}$ ) can change simultaneously. The monitoring of the subcriticality by the conventional inverse kinetics is difficult for such a simultaneous transient, because time variations of neutron count rate due to these changes cannot be distinguished in the conventional inverse kinetics method, *e.g.*, the neutron source strength and the point kinetics parameters are assumed to be constant. To address this problem, authors investigate the application of the particle filter (PF) method [1,2] and the time-domain decomposition based integral (TDDI) method [3] to the subcriticality measurement. The purpose of this study is to demonstrate the PF method via subcritical transient experiments conducted at the Kyoto University Criticality Assembly (KUCA). Although the reactor-noise measurements under the shutdown-state and the preliminary experiments of the TDDI method were also conducted, this report focuses mainly on the results of the PF method.

**METHODOLOGY:** In the case of the PF method, probability distributions of state variables (neutron number density  $n$ , delayed neutron precursor density  $C_i$ , effective neutron multiplication factor  $k_{\text{eff}}$ , source strength of external neutron source  $S$ , and neutron generation time  $\Lambda$ ) are approximated by histograms that consist of  $N$  particles having the state-variable vectors. Based on the state-variables at a previous times step, a priori histograms of the state-variables at next time step are calculated using the point kinetic equations. According to the time variation of measurement values (*e.g.*, neutron count rates), the histograms of state variables are successively updated based on the Bayes estimation. In this study, two detector-counts rates were utilized for the likelihood calculations to estimate simultaneously the changes of the reactivity  $\rho=(k_{\text{eff}} - 1)/k_{\text{eff}}$ ,  $S$ , and  $\Lambda$ : one is a  $\text{BF}_3$  counter to detect mainly fission neutrons; the other is a neutron rem counter for beam monitor. The likelihood function was assumed to be a bivariate normal distribution, where the diagonal components were statistical errors of count rates and the covariance was neglected. To estimate  $\Lambda$  from  $k_{\text{eff}}$ , the relationship between  $k_{\text{eff}}$  and  $\Lambda$  was approximated by a linear regression model, which was evaluated using the continuous energy Monte Carlo code, MCNP6.2 [4] with JENDL-4.0u [5] for various control rods patterns and the shutdown state in the EE1 cores. In the PF method, the system noises of  $\rho$  and  $S$  at each time step were set in proportion to differences of successive count rates of  $\text{BF}_3$  and rem counters, respectively. The system noise of  $\Lambda$  was determined by the prediction in-

terval of the linear regression model of  $\Lambda$  with respect to  $\rho$ .

**EXPERIMENTS:** The transient experiments were carried out in subcritical EE1 cores driven by a D-T neutron source. As shown in Fig. 1, two time-variations of neutron count rates [cps] in the 2520 HEU-plates core were measured using a  $\text{BF}_3$  counter at the axial center positions in the polyethylene-reflector region and the rem counter above the tritium target. At the time (i) shown in Fig. 1, the pulsed frequency of deuteron beam were changed from 20 to 100 [Hz]. Transients were given by inserting three control rods within the time-range between (i) and (ii). At the time (ii), 3×3 fuel and reflector assemblies were withdrawn for the shutdown. In the estimation of ( $\rho$ ,  $S$ ,  $\Lambda$ ) using the PF method, the time step  $\Delta t$  and the total number of particles  $N$  were set to 1 [s] and 10000, respectively.

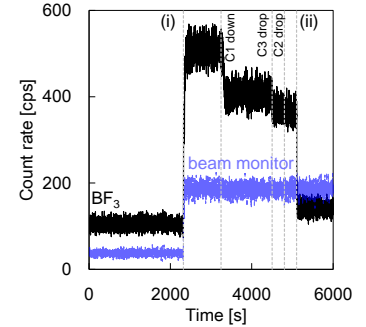


Fig. 1. Measured count rates.

**RESULTS:** The estimated results of  $\rho$  and  $\Lambda$  are presented in Fig. 2, where the reference values of  $\rho$  and  $\Lambda$  were numerical results evaluated by MCNP6.2 [4] with JENDL-4.0u [5]. Figure 2 shows that the estimated results of  $\rho$  and  $\Lambda$  agreed well with the reference values within  $2\sigma$  except for after the time (ii), even when  $S$  was changed. In this study,  $\Lambda$  was expressed by a simple linear regression model with respect to  $\rho$ ; thus, other measurements (*e.g.*, epithermal neutron count rate for spectrum index) may be useful to reduce the bias and uncertainty of the estimated results by the PF method.

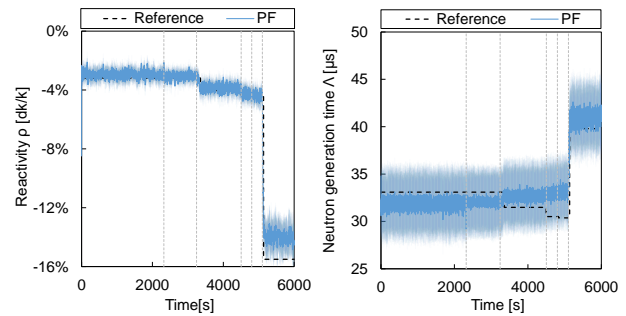


Fig. 2. Estimated results of  $\rho$  and  $\Lambda$  by PF method. Error bar represents  $\pm 2\sigma$  of  $N$  particles.

## REFERENCES:

- [1] G Kitagawa, J. Comput. Graph. Stat., **5** (1996) 1–25.
- [2] T. Ikeda, *et al.*, Trans. Am. Nucl. Sci., **118** (2018) 851–854.
- [3] A. Nonaka, *et al.*, Trans. Am. Nucl. Sci., **119** (2018) 1112–1115.
- [4] C.J. Werner (editor), LA-UR-17-29981 2017.
- [5] K. Shibata, *et al.*, J. Nucl. Sci. Technol., **48** (2011) 1–30.

# CO3-7 Sample worth measurements with systematically changed mixing ratios of Lead and Bismuth in A-core of KUCA for ADS

M. Fukushima<sup>1</sup>, A. Oizumi<sup>1</sup>, M. Yamanaka<sup>2</sup> and C. H. Pyeon<sup>2</sup>

<sup>1</sup>Nuclear Science and Engineering Center, Japan Atomic Energy Agency

<sup>2</sup>Institute for integrated Radiation and Nuclear Science, Kyoto University

**INTRODUCTION:** The Japan Atomic Energy Agency (JAEA) has investigated neutronics of the accelerator-driven system (ADS) of a lead bismuth eutectic (LBE) cooled-tank-type core to transmute minor actinides discharged from nuclear power plants. For the design study of ADS, integral experimental data of nuclear characteristics of LBE is necessary to validate cross sections of lead (Pb) and bismuth (Bi). In present study, sample worth measurements were carried out with systematically changed mixing ratios of lead and bismuth, which would be complementary to the previous data of Pb and Bi samples individually measured in FY 2013 [1] and FY 2017 [2], respectively.

**EXPERIMENTS:** The reference configuration had five test rods, which was the same one as the previous experiments. The test fuel rods were composed of 40 test cells with two HEU fuel plates (1/16 inch thick×2) and two Al plates (1/16 inch thick×2) as shown in **Figure 1**.

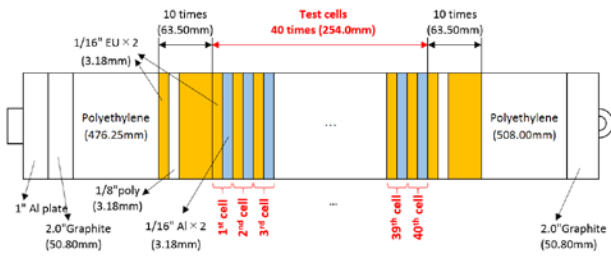


Figure 1. Schematic drawing of test fuel rod.

Table 1 Pattern of mixing ratios

Pattern	Mixing ratio Pb/(Pb+Bi)	# of plates		Cell locations with Pb plates*
		Pb	Bi	
1	100%	40	0	All cells
2	67.5%	27	13	1 <sup>st</sup> , 2 <sup>nd</sup> , 4 <sup>th</sup> , 5 <sup>th</sup> , ..., 37 <sup>th</sup> , 38 <sup>th</sup> , 40 <sup>th</sup>
3	50.0%	20	20	1 <sup>st</sup> , 3 <sup>rd</sup> , 5 <sup>th</sup> , ..., 37 <sup>th</sup> , 39 <sup>th</sup>
4	32.5%	13	27	3 <sup>rd</sup> , 6 <sup>th</sup> , 9 <sup>th</sup> , ..., 36 <sup>th</sup> , 39 <sup>th</sup>

\* Bi plates were loaded in the other cells.

In sample worth measurements, 80 plates of Al (1/16 inch thick) were replaced with a total of 40 sample plates of Pb or Bi (1/8 inch thick) per each test rod. The mixing ratio of Pb and Bi plates was systematically changed as shown in **Table 1**. The pattern 1 equivalent to the previous one [1] was carried out to check reproducibility of sample worth measurements. **Table 2** shows the experi-

mental results, together with the previous data for Pb and Bi samples individually. From the results of the pattern 1 (Pb:100%), good reproducibility was confirmed within experimental errors. **Table 2** also shows that the present results smoothly complement between two extremely data of the patterns 1 and 5. The sample worth measurements with systematically changed mixing ratios of Pb and Bi were successfully carried out from the viewpoint of reproducibility with the previous experiment.

Table 2 Experimental results

Pattern	Mixing ratio Pb/(Pb+Bi)	Measured reactivity worth (pcm)	
		Present	Previous
1	100%	156±4	156±8 [1]
2	67.5%	136±4	—
3	50.0%	124±4	—
4	32.5%	109±4	—
5	0.0%	—	84±3 [2]

**RESULTS:** Numerical analyses were preliminary conducted with MCNP6.1 together with JENDL-4.0 (J40) and ENDF/B-VII.1 (B71). The sample worth was estimated as the difference of the effective multiplication factors between the sample-loaded and reference configurations, without considering the criticality bias. **Figure 2** shows that the calculations by B71 agree with experimental data except for the pattern 1. On the other hand, the calculations by J40 overestimate for all the patterns. To clarify the cause of discrepancies in calculation accuracy between these libraries, nuclide-wise contributions were analyzed changing libraries from J40 to E71 for each nuclide. The discrepancies between them seem to be mainly due to differences in Al cross sections, not in Pb or Bi while the statistical errors should be still reduced.

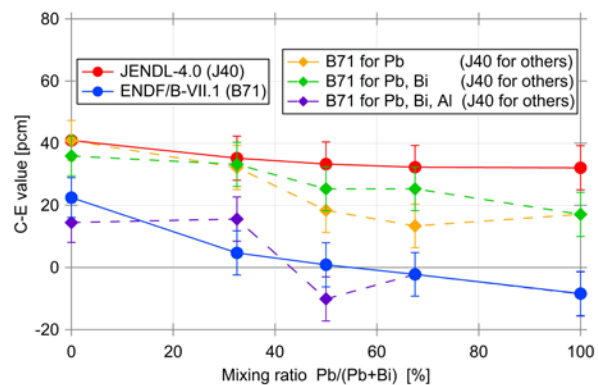


Figure 2. Calculation results (C– E values).

**REFERENCES:**

- [1] C. H. Pyeon, *et al.*, J. Nucl. Sci. Technol., **53**, 602-612, (2016).
- [2] C. H. Pyeon, *et al.*, J. Nucl. Sci. Technol., **55**, 1324-1335, (2018).

# CO3-8 Measurement of Neutron Reaction Rate on Accelerator-Driven System combined with DT neutron source

N. Aizawa, D. Maeda, A. Sekiguchi, H. Machiya, M. Yamanaka<sup>1</sup> and C. H. Pyeon<sup>1</sup>

Graduate School of Engineering, Tohoku University  
<sup>1</sup>Institute for Integrated Radiation and Nuclear Science, Kyoto University

**INTRODUCTION:** An accelerator-driven system (ADS) has been investigated to reduce the disposal burden of high-level radioactive waste by transmutation. The neutron reactions in the ADS core are dominated by neutrons with several MeV energy, but the contribution of several tens MeV neutrons to the reactions is not negligible. In addition, the multiplication factor  $k_{eff}$  ranges from 0.97 to 0.93 in the operation of an industrial scale ADS, and the influence of source neutrons on the total neutron multiplication is considered to vary with the multiplication factor. The experimental studies of the neutron reaction rates in the core region had been carried out in the previous studies with the use of KUCA A-core combined with DT (deuterium-tritium) neutron source [1-2]. DT neutron source is effective to examine the influence of the neutrons below 14 MeV. However, the subcriticalities set in the previous studies were very shallow (0.999 ~ 0.98 in  $k_{eff}$ ). The purpose of the present study is to examine the influence of the subcriticality on the neutron reactions through the foil activation method by changing the  $k_{eff}$  in range of the industrial-scale ADS operation.

**EXPERIMENTS:** The ADS experiment was performed in PE (polyethylene) moderated uranium core combined with DT neutron source. Figure 1 shows the core configuration. The fuel assembly (1/8"p60EUEU) was composed of 60 unit cells (unit cell: 1/8" PE plate + two 1/16" uranium plates). The subcriticality was set from 1396 to 8752 pcm (0.986 to 0.920 in  $k_{eff}$ ) by changing the number of fuel assembly. In, Al, Fe, Au foils were employed for the measurement of the neutron reaction

rates on the basis of the various reaction threshold energies, and were set at (M-O, 15), and In wire was set along (L-Z', 16-17) to measure the reaction rate distributions of  $^{115}\text{In}(n, \gamma)$ ,  $^{116m}\text{In}$  and  $^{115}\text{In}(n, n')$ , which were sensitive to thermal and the fast neutrons, respectively.

**RESULTS:** Figure 2 shows the reaction rates of each foil in the various subcriticalities. The measured reaction rates tended to decrease as the subcriticality became deeper due to the thermal power decrease. (The reaction rates of Al and Fe foils were not obtained due to the small thermal power in deep subcriticalities.) Their calculation/experiment values showed the almost stable values in the same trends as the previous studies. The one example of the measured reaction rate distributions is shown in Fig. 3. The peaks in  $^{115}\text{In}(n, \gamma)$ ,  $^{116m}\text{In}$  and  $^{115}\text{In}(n, n')$  were seen in the PE and fuel regions, respectively, and their distributions were considered to reproduce the thermal/fast neutron distributions well in the core. On the basis of the measured reaction rates, the effect of source neutrons on the reaction rates and the core characteristics is discussed as future works.

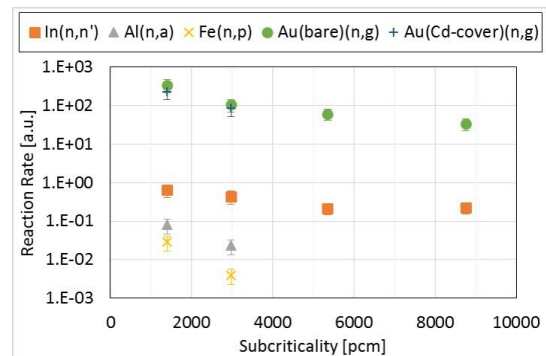


Fig. 2 Reaction rate variations with different subcriticalities

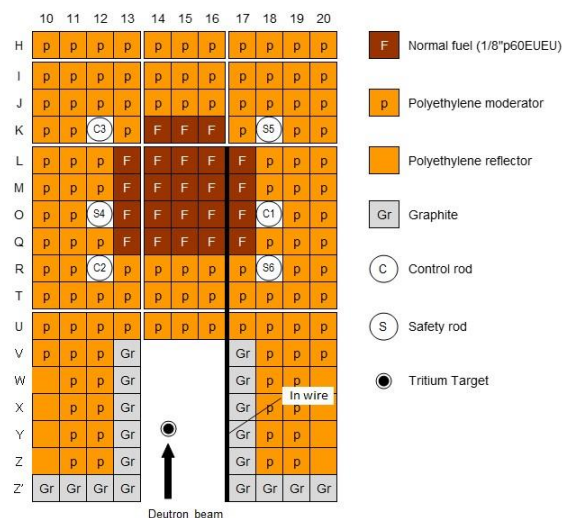


Fig. 1 Core configuration of KUCA A-core

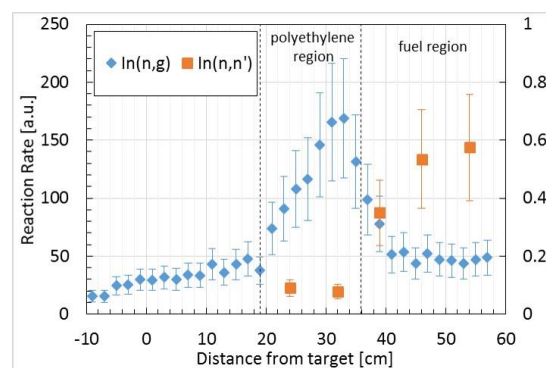


Fig. 3 Measured reaction rate distributions at the subcriticality of 2972 pcm

**REFERENCES:**

- [1] C. H. Pyeon, *et al.*, J. Nucl. Sci. Technol., **46**(10) (2009) 965-972.
- [2] C. H. Pyeon, *et al.*, Ann. Nucl. Ene., **40** (2012) 229-236.



# CO3-9 Reactor Noise Power-Spectral Analysis for a Graphite-Moderated and -Reflected Core

A. Sakon, K. Hashimoto, S. Hohara, K. Nakajima<sup>1</sup>,  
K. Takahashi<sup>1</sup>, Y. Fukaya<sup>2</sup>, and T. Sano<sup>3</sup>

Kindai University Atomic Energy Research Institute  
<sup>1</sup>Graduate School of Science and Engineering, Kindai University

<sup>2</sup>Sector of Fast Reactor and Advanced Reactor Research and Development, Japan Atomic Energy Agency

<sup>3</sup>Institute for Integrated Radiation and Nuclear Science, Kyoto University

**INTRODUCTION:** In light-water- or polyethylene-reflected thermal reactors, neutron detector for a reactor noise analysis must be placed closely to core region to observe neutron correlation information. In graphite-reflected thermal reactors, however, the detector may be placed far from the region. This is because mean free path of neutrons in graphite is longer than that in water or polyethylene. The objective of this study is experimentally to confirm a high flexibility of neutron detector placement in graphite reflector for reactor noise analysis.

**EXPERIMENTS:** The core configuration is shown in Fig. 1. “F” denoted a low-enriched fuel assembly, whose average enrichment is 5.41wt%. “D” is a driver highly-enriched fuel assembly. “G” is graphite reflector. Orange cell is polyethylene reflector. “1”, “2” and dots are BF<sub>3</sub> proportional neutron counters (1.0 in. dia., 15.47 in. len.). In a critical state, reactor noise analysis was carried out using BF<sub>3</sub> detector “1” and “2”. The distance from core region to detector “1” is about 35cm, and that to detector “2” is about 30cm.

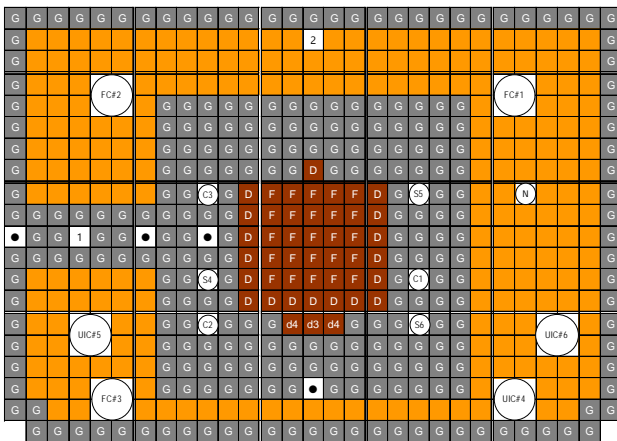


Fig. 1 Core configuration  
(B7/4”G2/8”p8EUNU+3/8”p38EU)

**RESULTS:** Auto-power spectral densities obtained from detector “1” and “2” are shown in Fig. 2 and Fig. 3, respectively. These figures also include least-squares fits of a conventional formula [1] to the spectral densities to determine the prompt-neutron decay constant  $\alpha_0$  ( $\beta_{\text{eff}}/\Lambda$ ), where the fitting was confined to a frequency range from 1.25 to 50 Hz. These derived decay constants  $67.9 \pm 8.2$

and  $63.3 \pm 14.5$  [1/s] were consistent with 63.1 [1/s] calculated by the continuous-energy Monte Carlo code MVP version 3 [2] within statistical uncertainty. As can be seen from these figures, however, the correlated component is being buried in the uncorrelated component and the fitting of Fig.3 is severer than that of Fig.2. This is because the detection efficiency of detector “2” is much lower than that of detector “1”. The lower efficiency is expected to be responsible for the two-layer polyethylene reflector between detector “2” and graphite reflector. It is confirmed that reactor noise analysis is possible using a detector placed at least 35cm far from core region. The further data analysis is in progress.

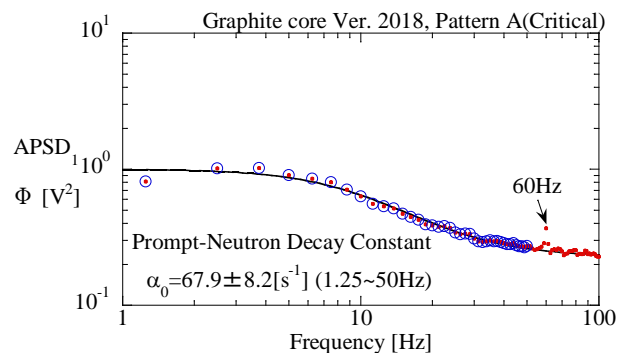


Fig. 2 Auto-Power Spectral Density (Detector “1”)

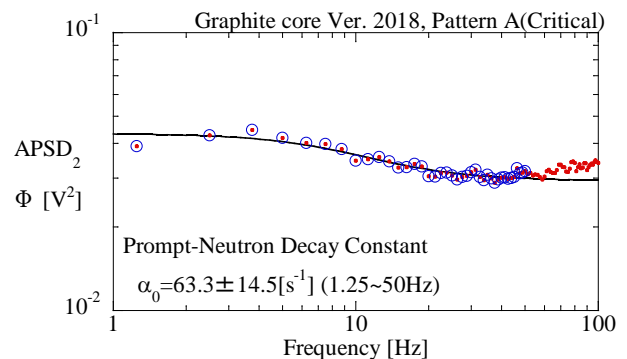


Fig. 3 Auto-Power Spectral Density (Detector “2”)

## REFERENCES:

- [1] M. M. R. Williams, Random Processes in Nuclear Reactors, (Pergamon Press, Oxford,1974), section 3.6.
- [2] Y. Nagaya, K. Okumura, T. Sakurai and T. Mori, MVP/GMVP Version 3 : General Purpose Monte Carlo Codes for Neutron and Photon Transport Calculations Based on Continuous Energy and Multigroup Methods, Tokai-mura: Japan Atomic Energy Agency; 2017, (JAEA-Data/Code 2016-018).

Y. Nauchi, S. Sato, M. Suzuki, T. Sano<sup>1\*</sup> and H. Unesaki<sup>1</sup>

Central Research Institute of Electric Power Industry  
<sup>1</sup>Institute for Integrated Radiation and Nuclear Science,  
 Kyoto University.

\*Current Affiliation: Atomic Energy Research Institute,  
 Kindai University.

### INTRODUCTION:

Application of the burn-up credit (BUC) is promising for efficient storage and transport of irradiated fuel. To take BUC, measurements are required to certify the residual fissile enrichment of the fuel. For a fresh uranium fuel, the  $^{235}\text{U}$  enrichment can be determined by measuring  $\gamma$  rays from decay of  $^{235}\text{U}$  and daughters of  $^{238}\text{U}$ . However, the method is not available for the irradiated fuel due to intense  $\gamma$  ray radiation from fission products (FP). The highest energy of FP  $\gamma$  ray is around 3.4 MeV. We have measured  $\gamma$  rays of 4.06 MeV from  $^{238}\text{U}(n,\gamma)$  reactions [1] and those of a continuum spectrum (3-8 MeV) from fission reactions [2]. Those  $\gamma$  rays might be measured for the irradiated fuel since the energy is higher than that of FP  $\gamma$  rays. Accordingly, the  $\gamma$  ray pulse height spectra were studied for subcritical cores of different  $^{235}\text{U}$  enrichment.

### EXPERIMENTS:

In the KUCA-A core, two kinds of subcritical cores of A1/8"p60EUNUNU and A1/8"p70EUNU fuel cells were mocked up with U-Al fuel plates of 93wt%  $^{235}\text{U}$  (EU) and the metal uranium of the natural enrichment (NU). The average enrichments of those were 3.1 and 5.4wt%, respectively. In the both cores, 14 fuel cells were loaded as shown in Fig. 1. The center of the core was void and the start-up neutron source of Am-Be was inserted. The fuel cells were surrounded by polyethylene and graphite cells. The  $\gamma$  rays from the  $^{238}\text{U}(n,\gamma)$  reactions and the fissions were measured with a HP-Ge detector of 30% relative efficiency. Between the fuel cells and the HP-Ge detector, polyethylene blocks of 35 cm thickness were loaded to shield the detector from the neutron irradiation. From the source, 4.44 MeV  $\gamma$  rays are radiated after de-excitation of  $^{12}\text{mC}$  produced by  $^9\text{Be}(\alpha,n)^{12}\text{mC}$  reactions. To reduce the 4.44 MeV  $\gamma$  rays from the source, Pb-Bi plates of 15.2 cm thickness is loaded.

### RESULTS:

In Fig. 2, the measured  $\gamma$  ray spectrum for A1/8"p60EUNUNU is shown. Different from the previous study where  $^{252}\text{Cf}$  was as the neutron source [1], the pulse height spectrum of  $\gamma$  rays from  $^{12}\text{mC}$  are significant in spite of the Pb-Bi shield. Another possible source of this component might be the inelastic scattering of  $^{12}\text{C}$  induced by the primary neutron from the Am-Be source since the average neutron energy of Am-Be is higher than that of  $^{252}\text{Cf}$  [3]. For all these  $\gamma$  rays from  $^{12}\text{mC}$  and the fission, the peak spectrum of 4.06 MeV was identified. The counting statistics of the peak are less than 11 % for the both cores. The fission  $\gamma$  ray spectra are overwrapped by those from  $^{12}\text{mC}$  below 4.5MeV. Then the relative fis-

sion  $\gamma$  ray count rates were assessed by integrating the spectrum over a region from 4.6 to 5.0 MeV. Then the count rate ratio of the 4.06 MeV peak to the fission was evaluated as listed in Table 1. The ratio decreases by 46% from A1/8"p60EUNUNU to A1/8"p60EUNU. The relative decrement is consistent with the variation of the number ratio of  $^{238}\text{U} / ^{235}\text{U}$  loaded in the two cores within the counting statistics of the  $\gamma$  rays. The consistent result indicates the feasibility to determine the enrichment  $^{235}\text{U}/\text{U}$  of fuel by the way of the neutron induced  $\gamma$  ray spectroscopy.

### REFERENCES:

- [1] Y. Nauchi *et al.*, KURRI progress report 2017 CO3-6, 2018.
- [2] Y. Nauchi *et al.*, Journal of Nuclear Science and Technology, 52(7-8), 1074-1083, 2015.
- [3] ISO-8259-1, 2001.

Magenta: fuel-cell, Yellow: Polyethylene, brown: graphite

N: Am-Be, White square: void cell

violet-circle: Pb-Bi is loaded at the same height with Am-Be

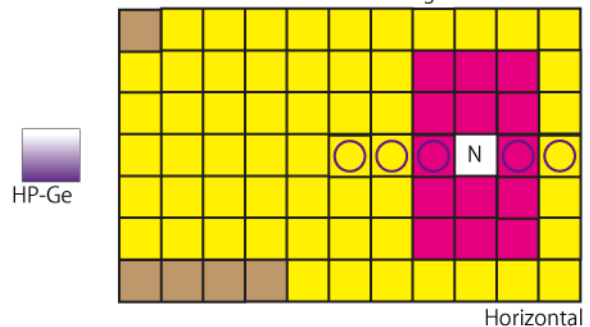


Fig. 1 Mocked up sub-critical core and detector.

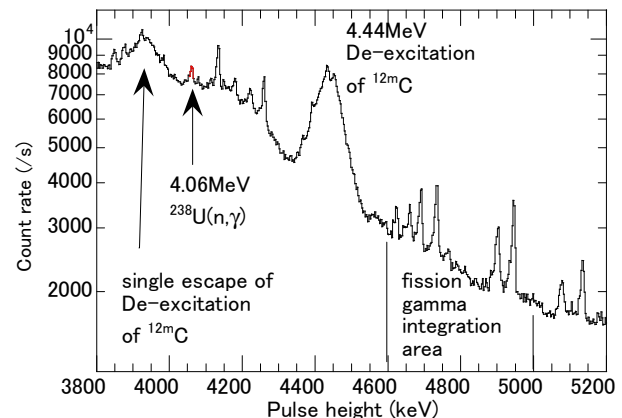


Fig. 2  $\gamma$  ray spectrum for core of 3.1wt%  $^{235}\text{U}$ .

Table 1 Count rate ratio of  $\gamma$  ray and  $^{238}\text{U}/^{235}\text{U}$

Fuel cell	Count rate ratio	Nuclide density ratio
	4.06MeV/fission	$^{238}\text{U}/^{235}\text{U}$
EUNUNU(3.1wt%)	0.00796	30.6
EUNU(5.4wt%)	0.00431	17.3
EUNUNU/EUNU	0.541	0.563

# CO3-11 Epithermal Neutron Capture Reactivity of Accident Tolerant Control Rod Materials

H. Ohta<sup>1</sup>, Y. Nauchi<sup>1</sup>, K. Nakamura<sup>1</sup>, S. Sato<sup>1</sup>, T. Sano<sup>2\*</sup> and H. Unesaki<sup>2</sup>

<sup>1</sup>Nuclear Research Technology Laboratory,  
Central Research Institute of Electric Power Industry  
<sup>2</sup>Institute for Integrated Radiation and Nuclear Science,  
Kyoto University  
\*Present affiliation: Atomic Energy Research Institute,  
Kindai University

**INTRODUCTION:** Since current control rods or blades for light water reactors (LWRs) using Ag-In-Cd alloy or B<sub>4</sub>C may be damaged and relocated from the core prior to serious fuel rod failure during severe accident (SA), the Central Research Institute of Electric Power Industry is developing an accident tolerant control rod (ATCR) applying the novel neutron-absorbing materials based on a mixture of RE<sub>2</sub>O<sub>3</sub>-MO<sub>2</sub> (RE = Sm or Eu, M = Zr or Hf). The ATCR improves the reactor shutdown margin and neutronic lifetime, and reduces the risk of re-criticality accident in any reactor conditions including SAs. A reactivity analysis of ATCR in the representative LWRs indicated that those candidate materials have enough reactivity worth comparable to or higher than the conventional neutron absorbing materials Ag-In-Cd alloy or B<sub>4</sub>C<sup>1</sup>. Furthermore, the reactivity worth of RE<sub>2</sub>O<sub>3</sub>-MO<sub>2</sub> in the thermal neutron field was validated with a criticality experiment<sup>2</sup>. In addition, the applicability of ATCR to the neutron spectrum hardening cores such as a mixed oxide fuel reactor is required in the future. This study aims to validate the epithermal neutron capture reactivity of RE<sub>2</sub>O<sub>3</sub>-MO<sub>2</sub>.

**EXPERIMENTS:** A critical core with thermal neutron spectrum (E3 core) was assembled in A-core of Kyoto University Critical Assembly (KUCA) as shown in Fig. 1. The unit cell of fuel assemblies is composed of a 93% enriched <sup>235</sup>U-Al alloy fuel plate of 2"×2"×1/16" and 3 polyethylene plates of 2"×2"×1/8"/plate. An Al-holder with an inner diameter of 1.2cm and a depth of 1.969cm lined with a 0.5 mm thick Cd foil, containing a mixed powder sample of RE<sub>2</sub>O<sub>3</sub>-MO<sub>2</sub> was loaded in the center of core. A prior analysis of neutron flux distribution by the continuous-energy Monte Carlo code MVP showed that low energy neutrons less than 0.25 eV are almost completely removed by the 0.5mm thick Cd lining, as shown in Fig. 2. The reactivity worth of each sample was measured with the period method and analyzed using MVP code with 2.58 billion neutron histories. The statistical error of

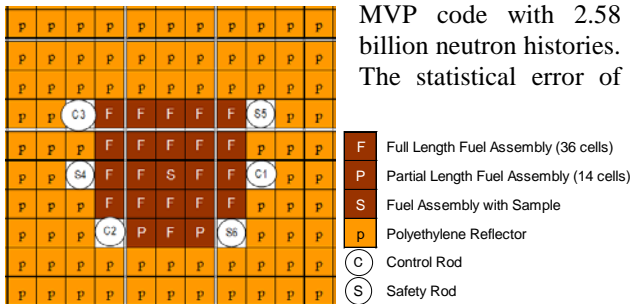


Fig. 1 Configuration of E3 core assembled in KUCA.

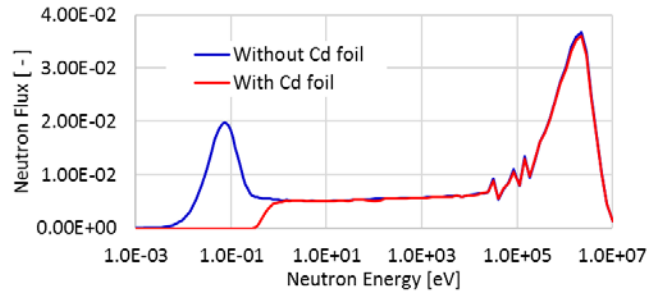


Fig. 2 Thermal neutron removal by 0.5mm thick Cd foil.

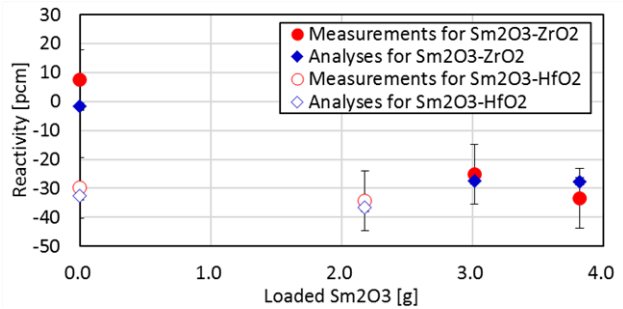


Fig. 3 Measurement and analysis results of reactivity for Sm<sub>2</sub>O<sub>3</sub>-ZrO<sub>2</sub> or Sm<sub>2</sub>O<sub>3</sub>-HfO<sub>2</sub>.

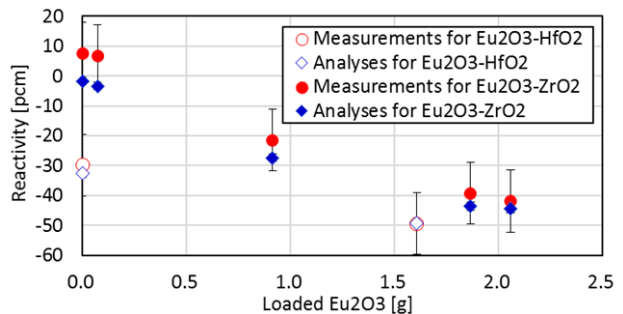


Fig. 4 Measurement and analysis results of reactivity for Eu<sub>2</sub>O<sub>3</sub>-ZrO<sub>2</sub> or Eu<sub>2</sub>O<sub>3</sub>-HfO<sub>2</sub>.

reactivity analysis was less than 1.5pcm. The neutron cross section libraries were generated using JENDL- 4.0.

**RESULTS:** The measurement results of the epithermal neutron capture reactivity for mixed powders of Sm<sub>2</sub>O<sub>3</sub>-MO<sub>2</sub> and Eu<sub>2</sub>O<sub>3</sub>-MO<sub>2</sub> are shown in Figs. 3 and 4, respectively in comparison with the analysis results. The experimental uncertainty of 10.4pcm was determined from the variation in 6 times measurements of the void sample reactivity. For all samples, the reactivity worth was predicted within the range of the experimental uncertainty. From these results, validity of neutron capture reactivity of Sm, Eu, Zr and Hf in the epithermal energy region was confirmed. As confirmed by the reactivity worth analysis in the mixed oxide fuel loaded LWRs, RE<sub>2</sub>O<sub>3</sub>-MO<sub>2</sub> is considered to be applicable as the alternative control materials.

[1] H. Ohta, *et al.*, *Top Fuel 2016*, 17556 (2016).  
[2] H. Ohta, *et al.* *Trans. 2018 ANS winter meeting*, Vol. 119, pp425-428 (2018).

## CO3-12 Reactor Physics Experiment in Graphite Moderation System for HTGR (I)

Y. Fukaya, S. Nakagawa, M. Goto, E. Ishitsuka, S. Kawakami, T. Uesaka, K. Morita, and T. Sano<sup>1</sup>

*Sector of Fast Reactor and Advanced Reactor Research and Development, Japan Atomic Energy Agency  
<sup>1</sup>Institute for Integrated Radiation and Nuclear Science, Kyoto University*

**INTRODUCTION:** The Japan Atomic Energy Agency (JAEA) started the Research and Development (R&D) to improve nuclear prediction techniques for High Temperature Gas-cooled Reactors (HTGRs). The objectives are to introduce generalized bias factor method [1] to avoid full mock-up experiment for the first commercial HTGR and to introduce reactor noise analysis to High Temperature Engineering Test Reactor (HTTR) experiment. To achieve the objectives, the reactor core of graphite moderation system named B7/4”G2/8”p8EUNU+3/8”p38EU (1) was newly composed in the B-rack of Kyoto University Critical Assembly (KUCA). The core plays a role of the reference core of the bias factor method, and the reactor noise was measured to develop the noise analysis scheme. In addition, training of operator of HTTR [2] was also performed during the experiments.

**EXPERIMENTS:** The core configuration is shown in Fig.1 “F” is the fuel assembly composed of 8 unit cells, which include a 1/16” thickness enriched uranium plate, a 1 mm thickness natural uranium plate, three 1/2” thickness graphite plates, a 1/4” thickness graphite plate, and two 1/8” thickness polyethylene plates, with axial graphite reflectors. The fuel plates (5.41 wt%) was designed to realize the averaged fuel enrichment of HTTR (5.9 wt%). The polyethylene plate was used to mimic the HTTR spectrum. “D” stands for the driver fuel assemblies composed of 38 unit cells, which include a 1/16” thickness enriched uranium plate, and, three 1/8” thickness of polyethylene, with axial graphite reflector. “d” stands for the partial length driver fuel to adjust criticality.

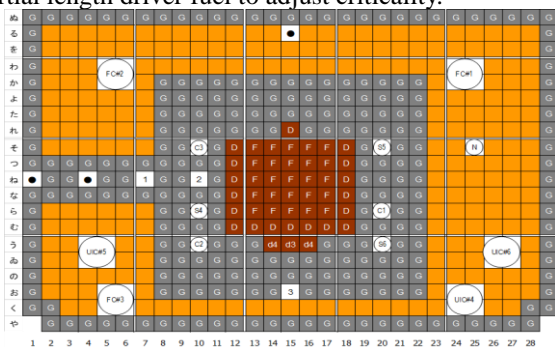


Fig. 1 Core configuration (Experiment)

**RESULTS:** Figure 2 shows the inverse count rate in an approach to criticality. The detector positions are slightly different with the experimental core shown in Fig.1. Calculated curve is also shown in the figure. The calculation is performed by MVP code which is neutron transport code based on Monte Carlo method with evaluated nuclear data library of JENDL4.0. The calculation curve is obtained only with considering multiplied neu-

trons. However, in the actual core, directly achieved neutrons from neutron source are also counted in the detectors. Therefore, the curves by the fission chamber from FC#1 to FC#3 are observed upper side of the calculated curve. The trend is significant for that of FC#1 because it is deployed near the neutron source. Finally, the core was reached to criticality with 930 enriched fuel plates and 7 steps of the approach to criticality.

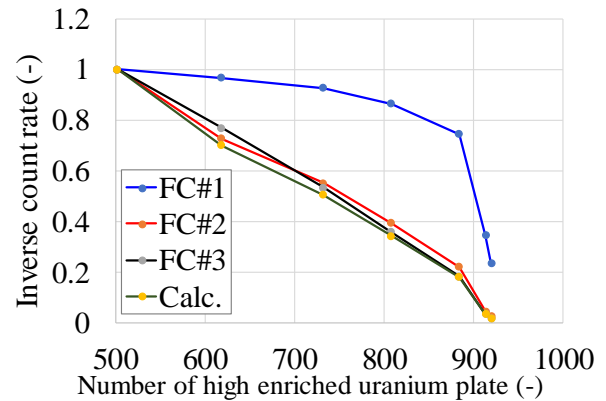


Fig.2 Inverse count rate

After that, reactivity worth of the core was measured. It is summarized in Table 1 with C/E values. The calculations were performed with JENDL4.0, ENDF/B7.0, and JEFF3.2. The experimental values were evaluated by period method for excess reactivity, by rod drop method for control rod, and center rack. Therefore, the C/E value of the center rack is large because the drop velocity of center rack is slow and against the assumption. For other reactivities, the calculations show a good agreement with the experimental values.

Table 1 Measured reactivity and C/E value

	Reactivity (%Δk/k)	C/E		
		J40	B70	F32
Excess	0.200	1.48	1.19	1.32
Control rod C1	0.871	1.22	1.23	1.20
Control rod C2	0.581	1.15	1.14	1.10
Control rod C3	0.530	1.13	1.12	1.14
Center core	1.813	2.15	2.13	2.13

By the calculation, the well thermalized neutron spectra in fuel assemblies were observed as well. Sensitivity coefficients similar to HTGR were expected to prepare the data base for the generalized bias factor method.

Moreover, reactor noise was also measured. Not only pulse signal for Feynman-α method, but also continuous signal for power spectrum method smoothed by pump circuit were measured.

### REFERENCES:

- [1] T. Sano, T. Takeda, J. Nucl. Sci. Technol.,43[12] (2006). 1465-1470.
- [2] E.Ishizuka, et al., University of Tokyo, UTNL-R 0499 (1969). 9-1.

T. Sano<sup>1,2</sup>, J. Hori<sup>1</sup>, J. Lee<sup>1</sup>, Y. Takahashi<sup>1</sup>, M. Yamanaka<sup>1</sup>  
C. H. Peyon<sup>1</sup>

<sup>1</sup>Institute for Integrated Radiation and Nuclear Science,  
Kyoto University

<sup>2</sup>Atomic Energy Research Institute, Kindai University  
(Apr. 2019~)

### INTRODUCTION:

In order to perform integral evaluation of neutron cross section for minor actinides (MAs), measurements of reaction rate ratios which are MAs/<sup>235</sup>U fission rate ratio and MAs/<sup>197</sup>Au at KUCA has been carried out [1]. The measured reaction rate ratio had been <sup>241</sup>Am/<sup>235</sup>U fission rate ratio, <sup>237</sup>Np/<sup>235</sup>U fission rate ratio and <sup>237</sup>Np/<sup>197</sup>Au capture rate ratio at various neutron spectrum fields, respectively. In those experiments, impurities, especially <sup>239</sup>Pu in the MAs has not been quantified, exactly. There is some possibility that the fission rate ratios has over estimated, because <sup>239</sup>Pu has very large fission cross section in thermal energy region.

Then, the <sup>241</sup>Am/<sup>235</sup>U fission rate ratio in KUCA A core was measured. The <sup>241</sup>Am sample which was quantified the amount <sup>239</sup>Pu as impurity.

### EXPERIMENTS:

An A1/8"p60EUEU core to measure the fission rate ratio was constructed at KUCA A core. A unit cell in the 1/8"p60EUEU fuel element has 2 enriched uranium fuel plates and 1 1/8" thickness polyethylene plate. The core has a void region in the center of core and the Back-to-back (BTB) fission chamber is inserted into the void region as shown in Fig.1. The <sup>241</sup>Am foil and <sup>235</sup>U foil were set in the BTB fission chamber. The sample information are shown in Table 1. <sup>239</sup>Pu in Am sample had been identified and quantified with TOF measurement at KURNS-LINAC [2]. Using BTB fission chamber, a MA foil and a <sup>235</sup>U foil are able to irradiate in the neutron spectrums, simultaneously.

In the experiment, the operational condition shows Table 2 and the irradiation time was 240 min.

### RESULTS:

Figure 2 shows the PH spectrum from the BTB fission chamber. In the figure, the signals from 500 to 3000 channel are due to <sup>241</sup>Am fission events. From those signals, the total fission events were  $58680 \pm 242.23$  counts. In the signal from <sup>235</sup>U, the total fission events of <sup>235</sup>U were  $1390521 \pm 1179.204$ . Then, the fission rate ratio of <sup>241</sup>Am/<sup>235</sup>U were observed as  $0.0422 \pm 0.0002$ . On the other hand, the fission rate ratio by numerical calculation with MVP3.0 and JENDL-4.0 was 0.0410. The C/E value was  $0.9722 \pm 0.42\%$ .

### REFERENCES:

- [1] H. Unesaki, Doctor Thesis, Nov. 2001 (2001).  
[2] T. Sano, 45th Summer Seminar of AESJ Reactor

Physics committee, (2016).

[3] Y. Nagaya, et. al., JAERI1348, JAEA, (2005).

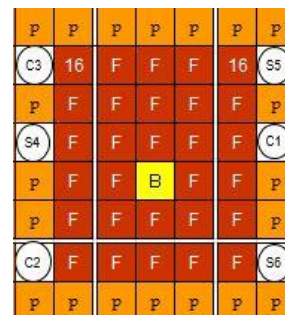
[4] K. Shibata, et. al., J. Nucl. Sci. Technol., 39(11), (2002)

**Table 1 Sample information [1]**

Sample	<sup>241</sup> Am		<sup>235</sup> U	
	Target Nuclide	<sup>241</sup> Am	$(1.73 \pm 0.02) \times 10^{16}$	<sup>235</sup> U
Impurities	<sup>239</sup> Pu	1.2ppm [2]	<sup>234</sup> U	470ppm
			<sup>236</sup> U	160ppm
			<sup>238</sup> U	400ppm

**Table 2 Operational data for sample irradiation**

Control Rod position (mm)	C1	714.93 mm
	C2	715.19 mm
	C3	715.24 mm
	S4, S5, S6	1200 mm
Core temperature (°C)		18.7 °C
Lin-N		$1 \mu\text{A} \times 35.2 \%$
Log-N		$2.9 \times 10^{-7} \text{ A}$
Gamma monitor		$2.3 \times 10^3 \mu\text{Sv/h}$



**F: 1/8"p60EUEU fuel element,  
16: 1/8"p16EUEU Partial Fuel element,  
p: 10" polyethylene reflector  
C: Control Rod, S: Safety Rod,  
B: Void region with BTB fission chamber  
Fig. 1 Core configuration**

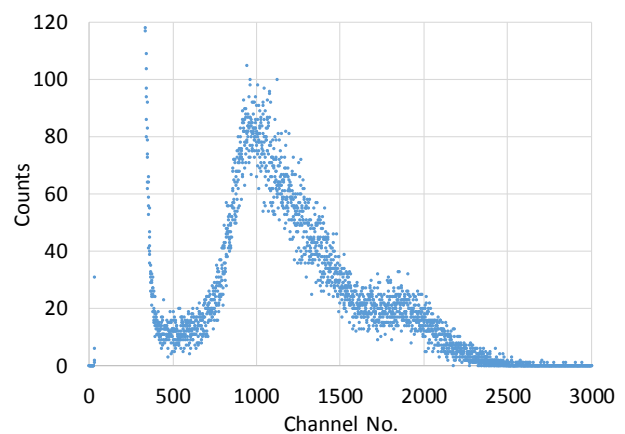


**Fig.2 PH spectrum from BTB chamber**

T. Sano<sup>1,2</sup>, H. Unesaki<sup>1</sup>, J. Hori<sup>1</sup>, J. Lee<sup>1</sup>, Y. Takahashi<sup>1</sup>,  
K. Takahashi<sup>3</sup>

<sup>1</sup>Institute for Integrated Radiation and Nuclear Science,  
Kyoto University

<sup>2</sup>Atomic Energy Research Institute, Kindai University  
(Apr. 2019~)

<sup>3</sup>Graduate School of Science and Engineering, Kindai  
University

## INTRODUCTION:

In order to perform integral evaluation of the <sup>232</sup>Th capture cross section, critical experiments with Th loaded various cores at KUCA has been carried out [1]. The H/<sup>235</sup>U nuclide ratio in those cores were about 150 – 315 to compensate the negative reactivity worth with Th loaded. The results of numerical analysis for the critical experiments showed magnitude of sensitivity coefficients respected for <sup>232</sup>Th capture cross sections in the thermal energy region larger than the resonance energy region. Then, a new critical experiment at KUCA B core which has about 70 of the H/<sup>235</sup>U ratio was carried out.

## EXPERIMENTS:

The new critical core consisted of two type fuel elements. One is Th loaded fuel element, and the other is driver fuel element. A unit cell of Th loaded fuel element has 3 enriched uranium (EU) plates with 1/16" thickness, 1 Th plate with 1/8" thickness and 2 polyethylene plates with 1/8" thickness. The one Th loaded fuel element has 27 unit cells. A unit cell of driver fuel elements consists of the 1 EU plate and the 2 polyethylene plates. The one driver fuel element consists of 49 unit cells.

Figure 1 shows the core configuration of the critical experiment. There were the 37 Th loaded fuel elements (F) and the 17 driver fuel elements (D). In addition, the partial driver fuel element which has 17 or 19 unit cells were loaded in order to adjust an excess reactivity worth of the critical core. Table 1 shows the critical data of the core.

## RESULTS:

First of experiments, the neutronics characteristics of the Th loaded core was measured to check on the parameters are fallen within the KUCA regulations. Table 1 shows the measured neutronics characteristics. The all characteristics are satisfied with the KUCA regulations.

In order to observe a effective multiplication factor ( $k_{eff}$ ) of the core, the excess reactivity worth was measured by the positive reactor period method. As the five-times-measured results, the evaluated excess reactivity worth was  $0.086 \pm 0.003$  (%dk/k) [2] and the  $k_{eff}$  was  $1.0009 \pm 0.0003$  [2]. Where, the kinetic parameters shown in Table 3 were calculated by MVP3.0 [3] and JENDL-4.0 [4].

## ARKNOWLEDGEMENT:

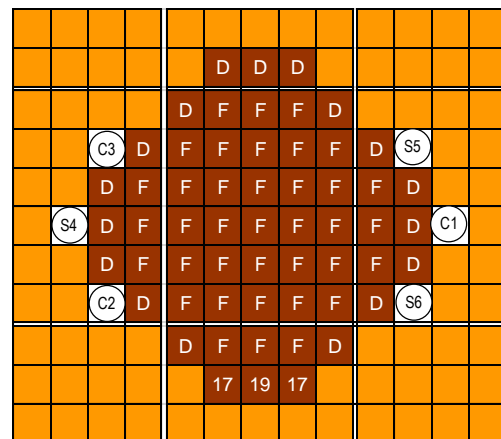
A part of the present study was supported by CHUBU Electric Power Co., Inc.

## REFERENCES:

- [1] H. Unesaki, Doctor Thesis, Nov. 2001 (2001).
- [2] T. Sano, et. al., Abstract of AESJ Spring meeting, 1J11, (2019).
- [3] Y. Nagaya, et. al., JAERI1348, JAEA, (2005).
- [4] K. Shibata, et. al., J. Nucl. Sci. Technol., 39(11), (2002)

**Table 1 Critical data of the Th loaded core**

No. of loaded EU plates		3883
No. of loaded Th plates		999
Control Rod position (mm)	C1	1201.15
	C2	1206.11
	C3	735.63
	S4, S5, S6	1200
Core temperature (°C)		20.3



**F: Th loaded fuel element, D: Driver Fuel element, 17, 19: Partial Driver Fuel element, C: Control Rod, S: Safety Rod**

**Fig. 1 Core configuration**

**Table 2 Measured neutronics characteristics of the Th loaded core**

Neutronics Characteristics	Charac-teristics	Measured (%dk/k)	KUCA Regulation
Excess reactivity (%dk/k)		0.086	< 0.35( %dk/k)
Rod worth (%dk/k)	C1 rod	0.244	Max. worth : < 1/3 of total worth
	C2 rod	0.379	
	C3 rod	0.430	
	Total*	(0.244+0.379+0.430)*2 =2.105	>Excess reactivity + 1 (%dk/k)
Center core worth (%k)		2.176	>1 (%dk/k)

\*S4, S5 and S6 rod worth are assumed same value as C1, C2 and C3 rods by symmetric geometry.

**Table 3 Kinetic Parameters**

$\beta_{eff}$	7.658E-3
$\Lambda$	3.257E-5

# CO3-15 Neutron measurement experiment using thin type experimental model of the SiC semiconductor detector

M. Nakano<sup>1</sup>, T. Saito<sup>1</sup>, Y. Harada<sup>1</sup>, T. Misawa<sup>2</sup>,  
Y. Kitamura<sup>2</sup>

<sup>1</sup>MITSUBISHI HEAVY INDUSTRIES, LTD.

<sup>2</sup>Institute for Integrated Radiation and Nuclear Science,  
Kyoto University

**INTRODUCTION:** The critical approach monitoring by neutron measurement is considered as one of the critical management methods in the institution which deals with nuclear fuels, such as a domestic nuclear power plant.

In this research, the experimental model of the SiC thin semiconductor neutron detector (called Test-rig in below section) with low gamma ray susceptibility can be used to carry out a neutron measurement examination in which neutron measurement is possible under high gamma ray environment.

When the characteristics of the Test-rig are evaluated, it is expectable to apply from now on as a neutron detector for a nuclear power plant or the fuel debris of a Fukushima Daiichi nuclear power plant.

**EXPERIMENTS:** As shown in Fig. 1, the reactor core which consists of a fuel bundle and a neutron source was created. The effective multiplication factor of the system at this time was estimated about as 0.93 as a result of the evaluation in an analysis code. The area from cell number "RA14" to "I16" was the space to set the Test-rig, neither fuel nor a polyethylene moderator had set. If this area was filled with polyethylene, the effective multiplication factor was estimated about 0.95.

The Test-rig was installed to the area from cell number "RA14" to "I16", and the neutron from the fuel cell was measured. In addition, a fuel cell and a polyethylene moderator were not set to "SO18" and "SO19" positions of Fig. 1, so that the neutron from the neutron source installed in the "SO20" position reaches a fuel cell directly.

**RESULTS:** The neutron of about 16,000 counts was measured by the measurement for about 3 hours using Test-rig, namely, sensitivity becomes about 1.34 cps. As a result, it has confirmed that the Test-rig has sensitivity equivalent to the sensitivity estimated in the Test-rig design. It shows that it is possible to measure enough neutrons for the sub-criticality monitoring, without needing gamma ray shielding under high gamma ray environment by manufacturing the SiC thin semiconductor neutron detector with which satisfies the requirement specification.

	7	8	9	10	11	12	13	14	15	16	17	18	19	20	21	22	23
KA	FC #2	2	2	2	2	2	2	2	2	2	2	2	2	2	2	2	FC #1
YO		2	2	2	2	2	2	2	2	2	2	2	2	2	2	2	
TA	2	2	2	2	2	2	2	2	2	2	2	2	2	2	2	2	2
RE	2	2	2	2	2	C3	2	2	F	2	2	S5	2	2	2	2	2
SO	2	2	2	2	2	2	F	F	F	F	F			N	2	2	2
TU	2	2	2	B	2	S4	F	F	F	F	F	C1	2	B	2	2	2
NE	2	2	2	2	2	2	F	F+	F	F	F+	2	2	2	2	2	2
NA	2	2	2	2	2	2	C2	F	F	F	S6	2	2	2	2	2	2
RA	2	2	2	2	2	2	2	ND			2	2	2	2	2	2	2
MU	2	2	2	2	B	2	2	ND			2	2	2	2	2	2	2
U	FC #3	2	2	2	2	2	2	ND			2	2	2	2	2	2	UIC #6
I		2	2	2	2	2	2	ND			2	2	2	2	2	2	
	7	8	9	10	11	12	13	14	15	16	17	18	19	20	21	22	23

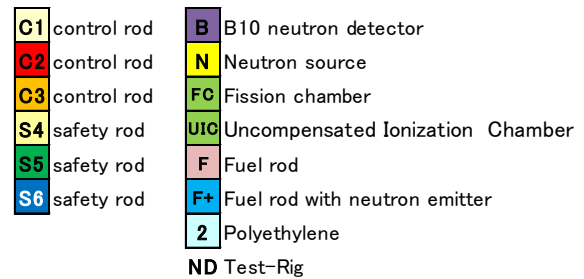


Fig. 1. Core of the neutron measurement examination

From now on, a SiC thin semiconductor neutron detector that satisfies the sub-criticality monitoring requirements can be made. The verification examination is continuously implemented as a neutron detector which can yield high sensitivity with high gamma ray extraction ratio, and application to the sub-criticality monitoring at nuclear power plants or Fukushima fuel debris retrieval work is expected.

## CO3-16 Verification of a method to estimate reactivity and fissile composition

Y. Yamane, S. Araki, Y. Kitamura<sup>1</sup>, T. Misawa<sup>1</sup>

Japan Atomic Energy Agency

<sup>1</sup>Institute for Integrated Radiation and Nuclear Science, Kyoto University

**INTRODUCTION:** The estimation of reactivity of an amount of unknown fissile material is one of important issues in the field of criticality safety.

JAEA has been theoretically developing a method to estimate the reactivity and composition of fissile isotope from neutron count rate alone[1-5]. The method is based on a newly developed equation of power in quasi-steady state after prompt jump/drop of power due to reactivity and/or neutron source change.

The purpose of the experiment is to obtain the experimental data for the verification and validation of the developed method. As the first step, the data for the estimation by using new method and other existing methods was obtained for comparison to each other. The reactivity estimation for a subcritical state close to critical one was focused for this time.

**EXPERIMENTS:** A subcritical core was made by removing fuel elements from the basic critical core configuration known as 3/8" p36EU of A-core. The tritium target irradiated with deuteron beam was used as the external neutron source.

BF<sub>3</sub> detectors were used. Figure 1 shows the core configuration and the position of the tritium target and BF<sub>3</sub> detectors.

The condition of deuteron beam was tuned so that the neutron count rate was suitable to Feynman- $\alpha$  method.

For the first 1000s, during 2000s and 3000s, in Fig.2, neutron count data was obtained under steady state. Then the deuteron beam was instantaneously cut off. After that, neutron count rate decreased and the measurement terminated in 500s after prompt drop of neutron count rate.

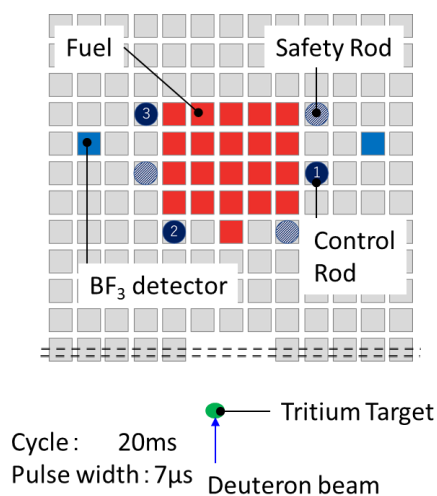


Fig. 1. Configuration of fuels and devices in A-core.

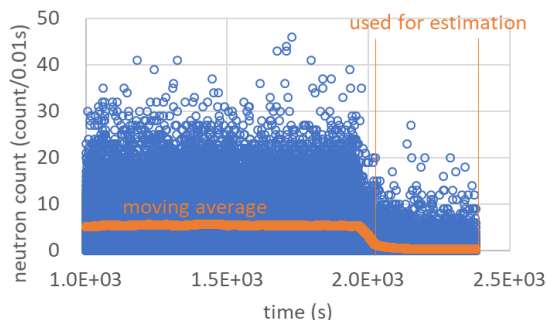


Fig. 2. Neutron count rate data. Blue circle shows neutron counts per 0.01s and orange line shows a profile of averaged neutron counts.

**RESULTS:** The estimated value obtained by applying the new method to the data was compared to the value calculated by using MVP code with JENDL-4.0 cross section library. The result is shown in Table 1, which shows that the range of C/E was 1.0 and 1.4[5-6]. The worse value was obtained for deeper subcriticality. The reason may be the lowness of the neutron count rate in the quasi-steady state compared to the estimation of TRACY experiment data.

The result indicates that estimated value of reactivity in dollar was reasonable in even not desirable condition in which neutron count rate was very low.

In next step, an experiment will be done in much better condition in deeper subcritical state.

Table 1. The comparison of reactivity values estimated by applying new method and calculated by using MVP code.

CORE	reactivity (\$)		C/E	initial count rate (cps)
	MVP	new		
KUCA	-0.49	-0.50	1.0	~50
	-1.0	-0.83	1.2	~30
	-1.3	-0.91	1.4	~20
TRACY	-1.4*	-1.3	1.1	~1000

\* not MVP, solution level difference method

### REFERENCES:

- [1] Y. Yamane, Proc. 2017 AESJ Spring meeting, 1F04, (2017) [in Japanese].
- [2] Y. Yamane, Proc. 2017 AESJ Fall meeting, 3G15, (2017) [in Japanese].
- [3] Y. Yamane, Proc. 2018 AESJ Spring meeting, 1F04, (2018) [in Japanese].
- [4] Y. Yamane, Proc. 2018 AESJ Fall meeting, 1M08, (2018) [in Japanese].
- [5] S. Araki, Y. Yamane, Y. Kitamura, T. Misawa, Proc. 2019 AESJ Spring meeting, 2J01, (2019) [in Japanese].
- [6] Y. Yamane, S. Araki, Y. Kitamura, T. Misawa, Proc. 2019 AESJ Spring meeting, 2J02, (2019) [in Japanese].



## CO3-17 Measurement of fundamental characteristics of nuclear reactor at KUCA (III)

Y. Kitamura<sup>1</sup>, T. Misawa<sup>1</sup>, Y. Takahashi<sup>1</sup>, Y. Hayashi<sup>2,3</sup>, Y. Morimoto<sup>2,4</sup>, M. Nakano<sup>2,5</sup>

<sup>1</sup>KURNS, <sup>2</sup>International Research Institute for Nuclear Decommissioning, <sup>3</sup>Toshiba Energy Systems & Solutions Corporation, <sup>4</sup>Hitachi-GE Nuclear Energy, Ltd. <sup>5</sup>Mitsubishi Heavy Industries, Ltd.

**ACKNOWLEDGEMENTS:** This work is a part of “Development of Technologies for Controlling Fuel Debris Criticality” project supported by the Ministry of Economy, Trade and Industry (METI).

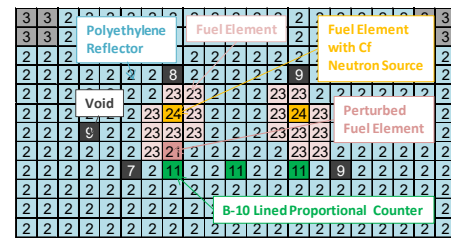
**INTRODUCTION:** The sub-criticality monitoring system for preventing criticality accident during fuel debris retrieval has been being developed by IRID[1]. This system is based on Feynman- $\alpha$  method[2]. The method is one of well-established sub-criticality measurement methods, but applicability for the sub-criticality measurement of fuel debris in Fukushima Daiichi Nuclear Power Plant is not demonstrated so far. The size of the fuel debris is one of the issues of the sub-criticality measurement. Investigation inside PCV revealed that the size of fuel debris reach approximately 5 meters. The one-point reactor approximation, which is assumed for the formulation of Feynman- $\alpha$  method, could not be valid for such large-scale system. So the sub-criticality may not be measured properly.

**EXPERIMENTS:** To investigate the applicability of the sub-criticality monitoring system of large-scale fuel debris, the following experiment was performed. It is known that the degree of flux tilt of large-scale system when a perturbation is added is correlated with the first order eigenvalue separation (E.S.)<sub>1</sub>, which is defined by the difference between the inverse of first order eigenvalue  $\lambda_1$  and the inverse of zeroth order eigenvalue  $\lambda_0$ [3]. Therefore, the first order eigenvalue separation (E.S.)<sub>1</sub> of experimental core was adjusted to simulate the one of large-scale system such as the fuel debris.

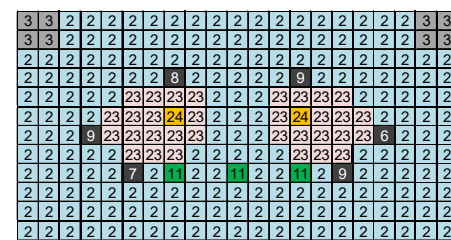
The examples of the core configuration are shown in Fig. 1. The core consists of two separated cores, and each core consists of several fuel elements and polyethylene reflectors. The first order eigenvalue separation (E.S.)<sub>1</sub> of the core was adjusted to same value (approximately 0.01) of the large-scale fuel debris to simulate it. The B-10 lined neutron proportional counters were set in front of the two separated cores. The neutron multiplication  $M(=1/(1-k_{\text{eff}}))$ , which is an indicator of sub-criticality, was measured with the prototype of the sub-criticality monitoring system, when the several type of perturbations that are assumed in fuel debris retrieval (e.g. replacement of low reactivity fuel element to high reactivity fuel element, replacement of fuel element to polyethylene reflector, etc.) were added to one of the two separated cores.

**RESULTS:** The result of the measurement of neutron multiplication  $M$  is shown in Fig. 2. The vertical axis of the graph represents measured neutron multiplication  $M_{\text{meas}}$ , the horizontal axis of the graph represents local

neutron multiplication  $M_{\text{local}}$  of one of the separated core, which is calculated with a Monte Carlo code, MVP[4]. The  $M_{\text{meas}}$  agreed well with the  $M_{\text{local}}$ . It is confirmed that the prototype of the sub-criticality monitoring system can be applicable for detecting approach to “local” criticality of large-scale fuel debris.



(a) Core 1 ( $k_{\text{eff}} \sim 0.8$ )



(b) Core 2 ( $k_{\text{eff}} \sim 0.95$ )

Fig. 1. Examples of core configuration

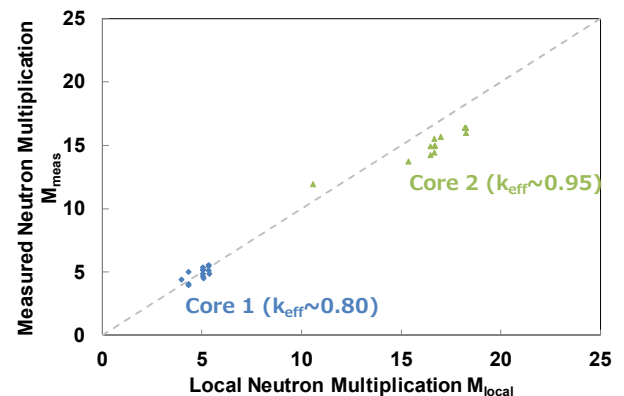


Fig. 2. Measurement results of neutron multiplication  $M$  of the cores that simulates large-scale fuel debris

### REFERENCES:

- [1] 2018. IRID Annual Research Report 2017, International Research Institute for Nuclear Decommissioning. 26-27. [http://irid.or.jp/\\_pdf/pamphleth29\\_eng.pdf](http://irid.or.jp/_pdf/pamphleth29_eng.pdf)
- [2] Feynman, R.P., de Hoffmann, F., Serber, R., “Dispersion of the neutron emission in U-235 Fission”, J. Nucl. Energy 3, 64-69 (1956).
- [3] K. Hashimoto, Ph.D. Thesis, Nagoya Univ. (1995).
- [4] Y. Nagaya *et al.*, MVP/GMVP Version 2 : General Purpose Monte Carlo Codes for Neutron and Photon Transport Calculations based on Continuous Energy and Multigroup Methods, Japan Atomic Energy Research Institute (2004).